

$$= \frac{\pi m v_F q_0^2}{2\hbar} \left[ 1 - \frac{2}{\pi} \tan^{-1} \left( \frac{2\hbar q_0^3 v_F}{\pi m \omega p} \right) \right].$$

In the limit of high magnetic fields, the Fermi velocity goes to zero and we have

$$I \approx \pi m^2 v_F \omega / \hbar^2,$$

$$\sigma(\omega)_{\text{nonres.}} = \frac{e^2 m \omega p^2 v_F n_i}{8\pi^2 \hbar^2 \omega^2 n}.$$

\* A portion of this work was done by Gregory Benford in partial satisfaction of the requirements for the Ph. D. at the University of California, San Diego.

† Present address: Cornell University, Ithaca, New York 14850.

<sup>1</sup>C. Oberman, A. Ron, and J. Dawson, *Phys. Fluids* **5**, 1514 (1962).

<sup>2</sup>R. Shanny, J. Dawson, and J. Greene, *Phys. Fluids* **6**, 1281 (1967).

<sup>3</sup>C. Oberman and F. Shure, *Phys. Fluids* **6**, 834 (1963).

<sup>4</sup>C. Oberman and A. Ron, *Phys. Rev.* **130**, 1291 (1963).

<sup>5</sup>O. Wolman and A. Ron, *Phys. Rev.* **148**, 548 (1966).

<sup>6</sup>N. Rostoker, *Phys. Fluids* **7**, 491 (1964).

<sup>7</sup>N. Rostoker, in *Proceedings of the Symposium in Applied Mathematics of the American Physical Society*, New York, 13–15 April 1965, edited by Harold Grad

(American Physical Society, Providence, R. I., 1967), Vol. 18.

<sup>8</sup>H. L. Berk, *Phys. Fluids* **7**, 257 (1964).

<sup>9</sup>D. F. DuBois, V. Gilinsky, and M. G. Kivelson, *Phys. Rev.* **129**, 2376 (1963).

<sup>10</sup>M. Rensink, *Phys. Rev.* **164**, 175 (1967).

<sup>11</sup>G. Benford and N. Rostoker, to be published.

<sup>12</sup>L. M. Roth and P. N. Argyres, in *Semiconductors and Semimetals*, edited by R. K. Willardson and A. C. Beer (Academic Press, Inc., New York, 1966), Vol. 1, p.159.

<sup>13</sup>We have assumed  $q_z$  and  $\omega$  greater than zero. For other values we use  $D(q_z, q_\perp^2, \omega) = D(-q_z, q_\perp^2, \omega) = D^*(-q_z, q_\perp^2, -\omega)$ . Also, since  $a^2 \rightarrow 0$  as  $B \rightarrow \infty$  we can set  $\exp(-\frac{1}{2}q_\perp^2 a^2) = 1$  to lowest order in  $(1/\omega_c)$ .

<sup>14</sup>M. J. Stephen, *Phys. Rev.* **129**, 997 (1963).

## Critical Velocity of a Superflowing Liquid-Helium Film Using Third Sound\*†

K. A. Pickar<sup>‡</sup> and K. R. Atkins

*Physics Department, University of Pennsylvania, Philadelphia, Pennsylvania*

(Received 30 September 1968)

An investigation of the critical velocity of the helium film is made by impressing a third-sound wave (surface ripple with van der Waals restoring force) on a superflowing film. The velocities of the wave are measured traveling upstream and downstream, and the superfluid critical velocity is deduced as  $V_c = \frac{1}{2}(U_3 \text{ down} - U_3 \text{ up})$ .

The critical velocity at the lowest temperature (1.25°K) as a function of the film height is found to be close to  $\hbar/2md$ , where  $d$  is the film thickness. This is compared with existing theories and is found compatible with the velocity necessary for the stability of a vortex-line-image pair with a separation of  $2d$ . Disturbing effects produced by the method used to excite the third sound make it impossible to measure the critical velocity at high temperatures. Arguments are advanced for believing that these disturbing effects do not invalidate the low-temperature results. Since the third-sound wave is formed by the longitudinal oscillation of the superfluid component, the observation of the wave in a film which is flowing at the critical velocity indicates the possibility of film velocities in excess of  $V_c$  for measured times  $T \sim 10$  msec, where  $T$  is half a third-sound period. This implies that there is a relaxation time  $\tau$  for the creation of vortices where  $\tau > T$ . From the data, an upper limit is placed on the difference in thickness between the flowing film and a static film.

### I. INTRODUCTION

The critical velocity of the liquid-helium film,

$V_c$ , flowing under a gravitational potential has heretofore been measured by examining the critical transfer rate  $\sigma = (\rho_s/\rho)V_c d$ , where  $\rho_s/\rho$  is the

ratio of superfluid to total fluid densities,  $V_c$  is the "critical velocity for film flow," and  $d$  is the film thickness at the narrowest constriction in the container above the highest liquid level. These measurements are characterized by a number of unexplained effects.<sup>1,2</sup> They are often not reproducible; different methods of filling the beaker give different results; the temperature variation is not as  $\rho_s/\rho$ ; small amounts of contamination on the surface and the nature of the surface itself affect the transfer rates, etc. Because of the wide variation in transfer rates, measurements of transfer rate and film thickness should be made with the same apparatus and preferably during the same run to obtain reliable critical-velocity estimates. Jackson and Grimes<sup>1</sup> measured the transfer rate with a stainless-steel beaker and at the same time determined the thickness of the flowing film on the outside of the beaker using an optical method. Their results give  $V_c = (\rho\sigma/\rho_s d) = 52.5$  cm/sec.

Atkins<sup>3</sup> also measured the transfer rate in his oscillating-film experiment to determine the film thickness. His results as calculated by Daunt and Smith<sup>4</sup> give at  $T = 1.47^\circ\text{K}$

$\sigma$ (cm <sup>2</sup> /sec)	$d$ (cm)	$V_c$ (cm/sec)
$7.4 \times 10^{-5}$	$1.9 \times 10^{-6}$	39
7.8	2.1	37
8.15	2.3	35

The velocity of the helium film over a copper spiral was measured by Knudsen and Dillinger<sup>5</sup> by determining the time it takes for a helium film to form a drop at the bottom end of a spiral along which the film flows. The velocity obtained was 37 cm/sec at  $1.3^\circ\text{K}$ . A later velocity reported by Dillinger<sup>6</sup> gives 17.7 cm/sec. These results do not exhibit the dependence of the velocity on film height. In addition, it is not clear that the velocity of an advancing front of the helium film is the same as the critical velocity obtained in film-transfer measurements.

Clearly, a direct measurement of  $V_c$  is desirable. We shall now describe how third sound provides a means to do this.

## II. THIRD SOUND

Third sound is a surface wave in the superfluid component of a liquid-helium film, the normal fluid remaining clamped to the wall. Its velocity  $U_3$  can be shown<sup>7</sup> to be

$$U_3^2 = \omega^2/k^2 = (\rho_s/\rho)df(1 + TS/L). \quad (1)$$

Here  $f$  is the van der Waals force of attraction per unit mass,  $T$  is the absolute temperature,  $S$  is the entropy per unit mass,  $L$  is the latent heat per unit mass. The factor  $TS/L$  is negligible at

$1.2^\circ\text{K}$  and gives a correction of only 10% near the  $\lambda$  point.

Third sound was detected by Everitt, Atkins, and Denenstein<sup>8</sup> by impressing a plane wave on the film and monitoring the oscillating film thickness at a distance from the excitation region using ellipsometric techniques. Their results in general corroborate Eq. (1). Recently, third sound in an unsaturated film has been investigated by Rudnick, Kagiwada, Fraser, and Guyon.<sup>9</sup>

The program in the present experiment was to impress a third-sound wave both upstream and downstream on a film flowing at the critical velocity. By measuring the new third-sound velocities  $U_{\text{down}}$  and  $U_{\text{up}}$  and assuming  $U_{\text{up}}^{\text{down}} = U_3 \pm V_c$  we obtain the first direct measurement of the steady-state critical velocity as  $V_c = \frac{1}{2}(U_{\text{down}} - U_{\text{up}})$ .

## III. APPARATUS

### A. Excitation and Detection

The system, described simply, consists of a stainless-steel strip  $\frac{3}{8} \times \frac{5}{4}$  in.<sup>2</sup> polished to  $0.1 \mu$  on which a superfluid liquid-helium film is constrained to flow at the critical velocity. A surface wave (third sound) is impressed on the moving film using an infrared chopper system similar to that described by Everitt *et al.*<sup>8</sup> Here the image of a strip filament is focussed on the mirror transverse to the direction of flow. The image may be chopped at up to 1200 Hz.

As shown in Fig. 1, the resulting wave is monitored by a detection system consisting of a plane-polarized strip of light incident on the mirror. The eccentricity of the resulting elliptically polarized light is modulated by the oscillating thickness of the film. This light is optically analyzed and passes into a phototube. The resulting signal is phase detected at the chopping frequency and integrated for a fixed length of time. The position along the mirror of the infrared exciting light is changed, and an integration of the phase analyzed signal performed at the new chopper-detector interval, etc. A wavelength is measured by examining the envelope of some 35 integrations, each performed every 0.05 cm. After one scan is taken over the entire mirror, the amplitude and phase of the axis-crossing regions are repeated. Only those measurements for which the crossovers do not shift in time are retained. The wavelengths are measured by tabulating peaks and crossovers, finding the differences between alternate crossovers and differences between adjacent peaks on the same side of the axis, averaging all these differences, and finding the standard deviation. The frequency of the wave is read directly from an oscilloscope using a photocell detector positioned in front of the chopping wheel.

This ellipsometric detection system is that of

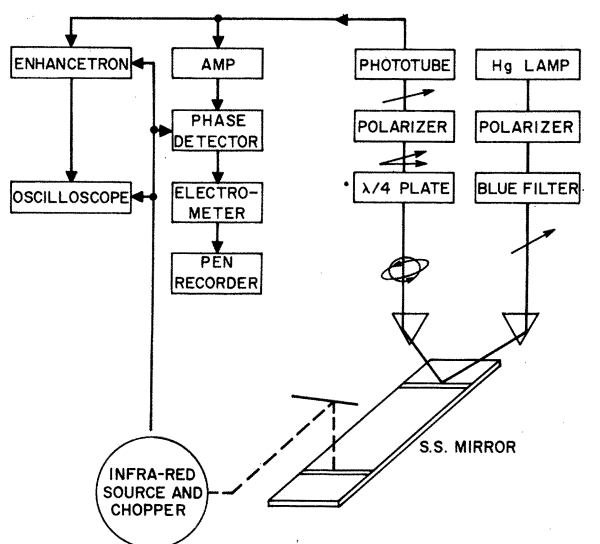


FIG. 1. Detection system showing how reflected polarized light is modulated by the changing thickness of the film and how resulting signal from phototube may be fed into either a multichannel analyser or a phase-detection system. For more details on optical and phase-detection system see Ref. 8.

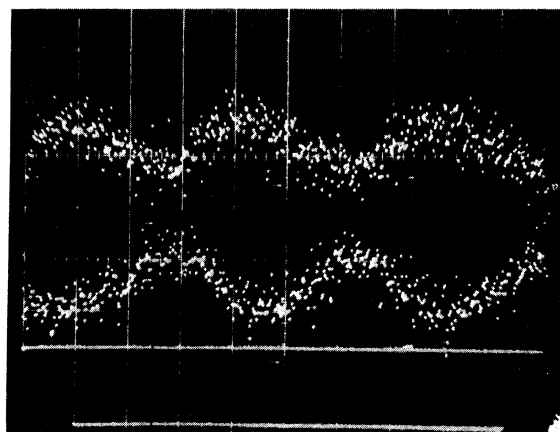


FIG. 2. Output of the multichannel analyser showing wave amplitude versus time for two different chopper positions. The observed waves are detected separately in alternate channels, stored, and then displayed on the scope simultaneously. A crude velocity measurement can be obtained by observing the advance in the peak on the time scale and dividing this number into the change in chopper position. Attempts were made to use this technique with third-sound pulses, but this did not prove to be as accurate as the phase-detection technique.

Everitt *et al.*, with two important exceptions. The phase detector originally employed was a 12-pole switch mounted on the shaft which turned the chopper disk. This proved mechanically unreliable and the present design uses two photoconductive cells placed opposite two light bulbs on either side of the chopper wheel. Such an arrangement gives a duty cycle close to 1, a factor of 2 better than mechanical switch method, as well as more reliable operation.

A second addition was an alternative method for observing the wave using an Enhancetron, a multichannel analyser, manufactured by the Nuclear Data Corporation. The signal from the phototube is fed directly into the Enhancetron which digitalizes and sums the information in each channel. The Enhancetron is triggered by an oscilloscope pulse which is phase-locked at the frequency of the chopper. The output of the Enhancetron may either be displayed and photographed off a second oscilloscope or read out on the recorder. This provides a picture of the wave as a function of time for a given position of the chopper. The Enhancetron method has the advantage of displaying the actual picture of the wave including information on higher harmonics and reflections, information which is suppressed in the phase detection method. Fig. 2 shows a typical Enhancetron output photographed off the oscilloscope. The two observed waves were integrated separately and represent two different chopper-detector distances.

### B. Inner Chamber Contents

The first attempts to measure the velocity of third sound in a moving film were made by Everitt *et al.*, by attaching heater wires around either end of a standard third-sound mirror. Current was passed through first one and then the other, and the difference in  $U_3$  was measured. The results, however, were inconclusive, as the measured wavelengths appeared to become large in the vicinity of the heater. This would suggest the film is thinner in that region because of the applied heat, thus causing the third-sound wave to flow faster. ( $U_3 \propto d^{-3/2}$ , where  $U_3$  is the third-sound velocity, and  $d$  is the film thickness.) It seemed clear that this was an unsatisfactory device to measure the critical velocity.

In its final form our apparatus was designed to: (1) channel the film so that laminar flow at the critical velocity would prevail in the region of interest, (2) maintain insofar as possible isothermal conditions between the wells.

The apparatus is shown in Fig. 3. It was constructed out of a  $1\frac{5}{8}$ -in. -diameter rod of E. T. P. copper to assure good thermal conductivity. Two holes were milled out from the bottom to  $\frac{1}{8}$  in. from the top to form the wells. Two  $\frac{3}{32} \times \frac{3}{8}$ -in.<sup>2</sup> slots were milled down from the top to form paths for the film. A stainless-steel strip polished to  $0.1 \mu$  was epoxied to the copper between the slots with Shell 828 resin and Shell Epon hardener.

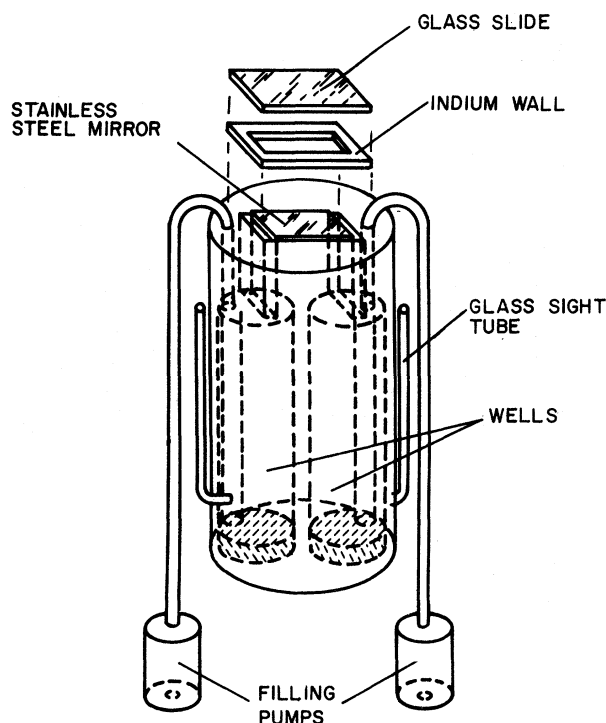


FIG. 3. Apparatus for channeling film flow from one well through a corridor with a glass "ceiling," indium "walls", and a polished stainless steel "floor" down into the other well. Both the chopper radiation and the detector light are projected through the glass "ceiling" onto the stainless steel "floor" on which the wave is generated and detected.

This epoxy proved to have good temperature-contraction properties and maintained a superleak-proof seal at 1.2°K for metal-metal and even glass-metal bonds. A rectangular ring of indium wire of cross-section  $\frac{1}{16} \times \frac{1}{16}$  in.<sup>2</sup> was epoxied around the stainless-steel strip and slots. A glass slide with an antireflection coating was epoxied on top of the indium ring. It was arranged so that the perimeter for film flow through this "tunnel" would be smaller than the perimeter of the slots. Since the film reaches its critical velocity at the smallest perimeter above the highest bulk level, we expect that the critical velocity is attained as the film flows across the mirror.

The helium levels in the wells were read using glass sight tubes. The wells were individually filled using fountain-effect filling pumps, which are stainless-steel tubes packed at the bottom with cleaned lamp black in which 10- $\Omega$  heaters are buried. Two mW is enough to build up a large thermomechanical pressure head. The tubes widen out to  $\frac{1}{4}$  in. inside the wells to prevent the formation of siphons that would empty the wells. The apparatus is supported by a three-screw suspension descending from the prism mounts.

The apparatus and the prisms with their supports are encased in a glass cup joined to a copper disk by an indium pressure seal (not shown). The copper disk is supported by the light tubes. This inner chamber then forms a separate vacuum system surrounded by the 3-in. helium Dewar.

### C. The High-Vacuum System

It was seen in the course of the present experiments that the third-sound velocity and the repeatability of this velocity were very much dependent upon the cleanliness of the mirror surface. This result was not seen in the previous experiment of third sound on a static film in which surface cleanliness appeared not to play a major role.

Obviously the flow velocity as well as the film thickness is affected by the cleanliness of the surface.<sup>1</sup> The contamination could be divided into three classifications: (1) the residue of the solvent left in the original cleaning of the mirror surface, (2) the pollutants which collect from run to run (e.g., water vapor, vacuum-pump oil, dust from improper trapping, leaks, etc.), and (3) condensed air residue resulting from pumping to an insufficient vacuum before cooling down.

The scatter in data taken in one run was very large, as much as 50%, when the surface was not clean for any of these reasons. In addition, the third-sound velocities were lowered by as much as one third when dirty conditions prevailed. To reduce cleaning-fluid residue, the mirror was vapor degreased in isopropyl alcohol before epoxying on the cover slide. To reduce the effect of accumulating pollutants, the system was kept pumped out to  $10^{-7}$  Torr with a well-trapped diffusion pump between runs. Care was taken to ensure that the system was leaktight, and the helium Dewar was kept at atmospheric pressure with gaseous helium between runs. The low pressure attained also served to eliminate any effect from condensed air on the mirror. In addition, the lamp black in the fountain effect pumps was heated to 400°C for several hours in a helium atmosphere to drive out volatile pollutants which might have found their way onto the mirror during outgassing. Allowing the lamp black to cool to room temperature in the helium atmosphere after heating assured that the adsorbed gas liberated from the carbon particles during outgassing would be helium and therefore would not contaminate the surface.

## IV. RESULTS

### A. The Dependence of the Critical Velocity on Level Difference

Consider Fig. 4. The movable chopper light is scanned along the mirror from the fixed detector-light position to the inner edge of well 2. An integration is performed every 0.5 mm. Because of the geometry, waves are only examined traveling

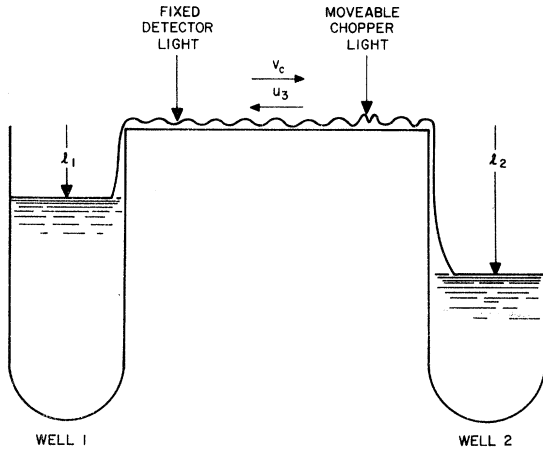


FIG. 4. Schematic diagram of apparatus showing helium draining from well 1 into well 2 through film flow and a third-sound wave traveling in the opposite direction to the film flow.

on the well-2 side of the detector light, as there is not enough space on the well-1 side to obtain accurate wavelengths. In the configuration shown, the wave is traveling upstream, since the level in well 1 is higher than the level in well 2. To obtain a downstream velocity measurement, helium is pumped into well 2 until  $l_2 < l_1$ . Twenty minutes are allowed for thermal equilibrium before a measurement is begun.

One might expect that the film velocity would be relatively insensitive to the pressure gradient  $|l_1 - l_2|$ , driving the film flow. We plot  $U_{\text{down}}$  and  $U_{\text{up}}$  against  $|l_1 - l_2|$  in Fig. 5. In this graph the circles are plots against  $|l_1 - l_2| = \Delta l$  with  $l_1$  left constant at approximately  $1.0 \pm 0.2$  cm and with the level in well 2 below the level in well 1. We see that the upstream third-sound velocity is constant in  $\Delta l$ . This suggests that  $V_c$  itself is constant in  $\Delta l$ . For the downstream results, however, with  $l_2$  left constant and the level in well 1 now below that in well 2, we see a very marked dependence of  $U_{\text{down}}$  on  $\Delta l$ . Here the open triangles are downstream third-sound velocities for  $l_2 = 5.7 \pm 0.5$  cm. The closed triangles are downstream velocities for  $l_2 = 1.2 \pm 0.3$  cm. It is highly unlikely that the increase in velocity with level difference (by a factor of 3) is due to a great increase in the critical velocity as  $\Delta l$  is changed. It is more likely that it is  $U_3$  itself which is changing. Since  $U_3 \sim d^{-3/2}$ , it is probable that the film is simply getting thinner as the level in well 1 is lowered even though the level of the source well, well 2, is kept constant. Indeed, if we now plot  $U_{\text{down}}$  against  $l_1$  independent of  $l_2$  (keeping the level in well 2 below that in well 1) we see as shown in Fig. 6 that within experimental error, the points with  $l_2 = 1.2 \pm 0.3$  cm now lie on the

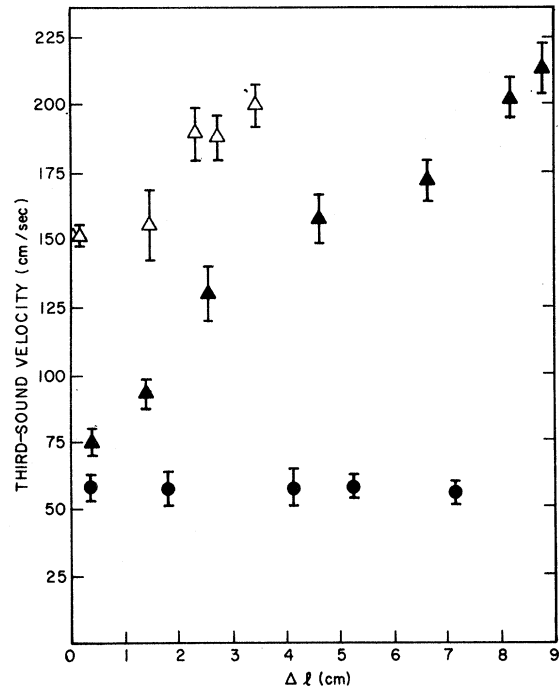


FIG. 5. Third-sound velocity ( $U_3$  down or  $U_3$  up) versus pressure gradient ( $|l_1 - l_2|$ ). The circles are plots of  $U_3$  up versus  $\Delta l$  for  $l_1 \approx 1$  cm. The solid triangles are plots of  $U_3$  down for  $l_2 \approx 1$  cm. The open triangles are  $U_3$  down for  $l_2 \approx 5.5$  cm. Here the height of one of the wells (the source well) is fixed, and the height of the other well (the sink well) is varied.

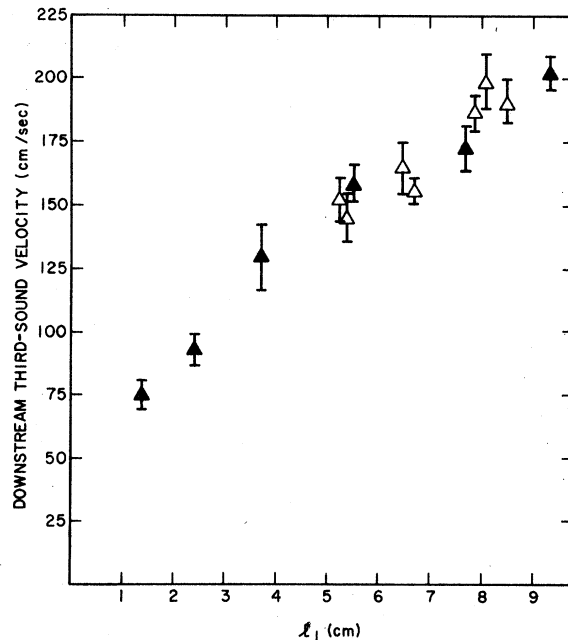


FIG. 6. Plot of  $U_3$  down versus  $l_1$ . Well 1 is the sink well in this case and well 2 is the source well.

same curve as the points with  $l_2 = 5.7 \pm 0.5$  cm. From this we are led to the conclusion that the thickness of the film in the region of interest (the region between chopper and detector) depends only upon the height  $l_1$ .

We must emphasize at this point that the apparatus is believed to be symmetric in its construction. The measured cross-sections of the two wells, for instance, are within 0.5% of one another. The only asymmetry introduced is that the chopper is only on the side near well 2, and the detector is only on the side near well 1. It is reasonable to assume then that the chopper is causing the thickness of the film in the region of interest to decouple from any dependence on well 2. This well is then relegated to the role of source or sink for the flowing film. This is not a small effect; the differences in film thickness which occur because the film depends on  $l_1$  instead of  $l_2$  are as much as one third the total film thickness.

Analogous phenomena are found in the literature. In a Jackson and Grimes experiment involving film flow out of a cylindrical beaker,<sup>1</sup> drops were seen to run down the outside of the vessel when the beaker was filled so that the inner level was less than 1 cm from the rim. They suggest that the flow rate depends on the thickness of the film on the inside of the beaker rim. If the thickness on the outside of the beaker depends only on the outside level (and is hence thinner), drops will form to carry off the excess flow. Consequently, one expects that in this geometry there is a discontinuity in the film thickness at the rim.

The potentiometer experiment of Keller and Hammel<sup>10</sup> shows that there is a discontinuity in the chemical potential of the film as the bulk fluid drops below a constriction giving a film-thickness discontinuity at the constriction.

#### B. The Dependence of Critical Velocity on Film Height

We can obtain consistent results by plotting third-sound velocity for the upstream and downstream cases as a function of the height  $l_1$ . The results at the lowest temperature  $T = 1.25^\circ\text{K}$  are shown in Fig. 7. Here the solid line is the velocity of third sound in a static film against film height as measured by Everitt *et al.* The data show the  $\sim 10\%$  scatter characteristic of film flow measurements but lie fairly symmetrically about the static  $U_3$  curve. The critical velocity as a function of film height is shown in Fig. 8 as taken from the data exhibited in Fig. 7.<sup>11</sup> The points are those measurements for which upstream and downstream third-sound velocities were taken consecutively and for which the wavelength varied by less than 5% across the mirror. The solid line is taken from one half the difference between the somewhat arbitrarily chosen "best" curves that

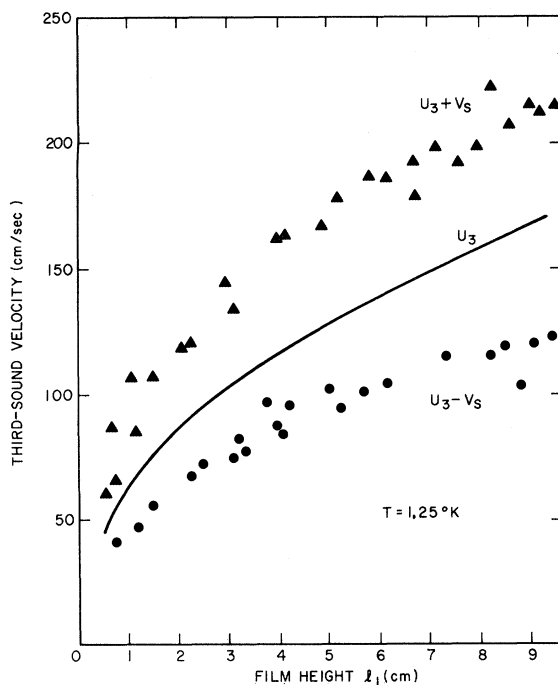


FIG. 7. Velocity of third sound upstream ( $U_3 - V_s$ ) and third sound downstream ( $U_3 + V_s$ ) against film height ( $l_1$ ). The solid curve is taken from the data of Everitt *et al.* for third sound in a static film.

can be drawn through the data in Fig. 7. The dotted line is  $\hbar/2md$  which may be derived from several theories. The open circle is Jackson and Grimes's<sup>1</sup> result taken at  $1.6^\circ\text{K}$ . The triangles are taken from Atkins's results for the oscillating film as calculated by Daunt and Smith.<sup>4</sup>

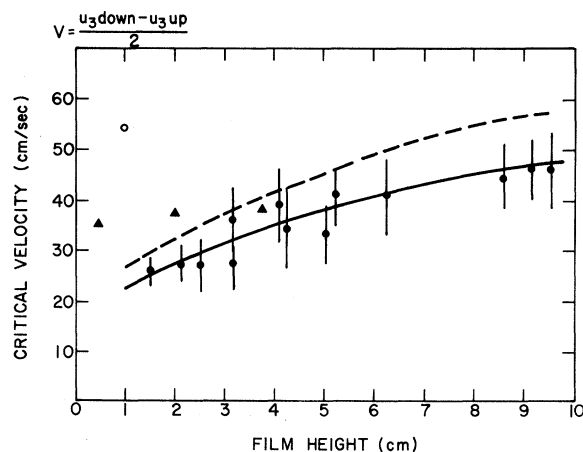


FIG. 8. Critical velocity versus film height ( $l_1$ ). The open circle is Atkins's result. The triangles are from Jackson and Grimes's results. The solid circles are from the present data. The dashed line is  $\hbar/(2md)$  and the solid line is  $\frac{1}{2}$  the difference between the curves best fitting the data in Fig. 7.

In an attempt to calculate  $V_c$ , Fetter<sup>12</sup> has considered the problem of a quantum-mechanical vortex-image pair created at a plane wall, but is unable to obtain a solution for the energy when the boundary condition that the wave function should vanish at the wall is applied. For the case of a vortex ring in a tube, however, he is able to calculate the energy. Taking the classical vortex-ring momentum and using the Landau criterion<sup>13</sup> he gets

$$V_c = \epsilon / p \simeq \hbar / 2mR, \quad (2)$$

where  $R$  is the radius of the ring and is assumed to be equal to the radius of the tube. If we set  $R$  equal to the thickness of the film, we get good agreement with the present experiment. Obviously, the geometries are quite different, but when one tries to apply the proper geometry of a vortex pair at a plane wall one finds that the Landau criterion gives a critical velocity that is much too high because of the very small values of momentum obtained when the vortices are closely spaced. This suggests that the vortex may be created away from the wall.

A very simple approach is to consider the motion of a vortex pair in an unbounded fluid. For the separation distance  $2C$  to remain constant, the pair must move with a translational velocity with respect to the background fluid of

$$V = \kappa / 4\pi C,$$

where  $\kappa$  is the circulation  $h/m$ . Thus, a single vortex near a wall will be in equilibrium with its image providing the background superfluid film moves at a velocity of  $V = \kappa / 2\pi C$ , where  $C$  is the distance of the vortex from the wall. If we set  $c = d$ , the film thickness, then the velocity of the film necessary for stability of the vortex pair would be very close to the critical velocity measured in this experiment. The placing of the vortex at the equilibrium surface of the film would, of course, produce a distortion in the film surface and require a corresponding increase in surface-tension energy. This increase is greater than the energy of the vortex pair itself. Such a "wash-board" configuration of the film surface has previously been proposed by Kuper<sup>14</sup> as a consequence of his assumption that the vortices form rows similar to a classical Karman vortex street.

#### C. Film Thickness

We have assumed that

$$U_{3 \text{ down}} = U_3' + V_c, \quad (3)$$

$$U_{3 \text{ up}} = U_3' - V_c. \quad (4)$$

Adding the equations

$$U_3' = \frac{1}{2}(U_{3 \text{ down}} + U_{3 \text{ up}}). \quad (5)$$

But  $U_3'$  does not necessarily have to be identical with the velocity of third sound in a static film if the thickness of a flowing film is different from that of a film at rest. This is because  $U_3$  is a function of film thickness

$$U_3^2 = (\rho_s / \rho) 3\alpha / d^3, \quad (6)$$

where  $\alpha$  is the van der Waals constant. Thus, we may use third sound as a probe to deduce any gross effect of motion on the film thickness.

Kontorovich<sup>15</sup> has calculated the effect of a kinetic energy term on the profile of the film and found the flowing film to be thinner. His results may be expressed<sup>16</sup> as

$$\delta d = V_c^2 d / 6gH \quad (7)$$

at the lowest temperature. To determine the effect on  $U_3$ , we differentiate the third-sound equation, substitute for  $\delta d$ , and rearrange terms to get

$$\delta U_3 / U_3 = V_c^2 / 4gH. \quad (8)$$

In Fig. 9 the full curve represents measurements<sup>8</sup> of  $U_3$  for a supposedly static film (Everitt *et al.*) and the dashed curve is derived from this by applying the Kontorovich correction of Eq. (8). The dotted curve represents the average of our measured upstream and downstream velocities. The difference between the three curves is not significantly larger than the scatter of the data and so our experiments do not resolve this point. However, we may conclude from our data that the thickness of the moving film is thinner than the static film by no more than the amount predicted by Kontorovich [Eq. (8)]. Substituting the values experimentally determined for  $V_c$ , we get  $\delta d/d < 4.2\%$  at  $h = 9$  cm,  $\delta d/d < 9.0\%$  at  $h = 1$  cm. The only previous work<sup>17</sup> on the thickness of a moving film gave  $\delta d/d = 5.6\%$  at  $1.68^\circ\text{K}$ ,  $h = 1$  cm.

#### D. Temperature Variation

When  $U_{3 \text{ down}}$  and  $U_{3 \text{ up}}$  are plotted as a function of temperature (Fig. 10) at  $l_1 = 5.4$  cm, we find the velocities converging as the temperature is raised. At  $2.0^\circ\text{K}$ , the difference between  $U_{3 \text{ up}}$  and  $U_{3 \text{ down}}$  becomes zero. At this temperature  $\rho_s / \rho$  in the bulk liquid  $\sim 0.5$ . This effect is less pronounced in thick films as shown in Fig. 11. Here  $(U_{3 \text{ down}} - U_{3 \text{ up}})$  appears constant below  $1.83^\circ\text{K}$ , converging only above this temperature. The third-sound waves observed

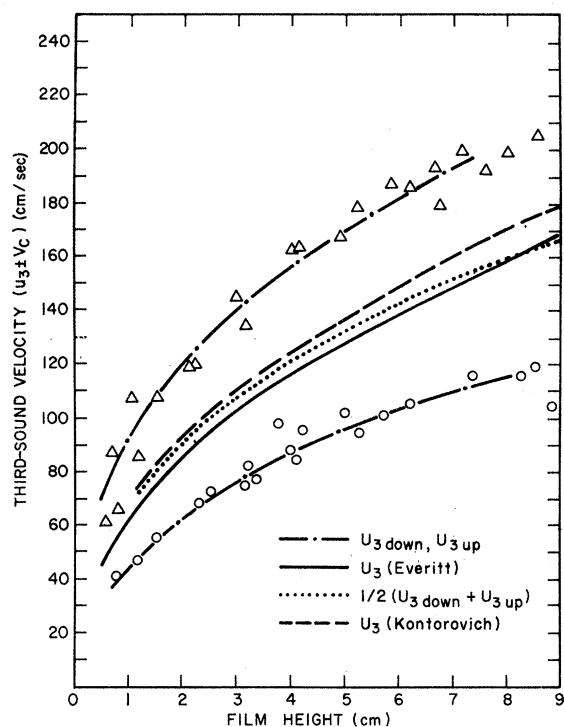


FIG. 9. Third-sound velocity versus film height ( $l_1$ ). The dotted curve is somewhat arbitrarily drawn from  $\frac{1}{2}(U_3 \text{ up} + U_3 \text{ down})$ . The triangles and circles are third sound downstream and upstream, respectively.

at these high temperatures exhibit a very good signal-to-noise ratio, large attenuation ( $\sim 0.3$  per wavelength), small amplitude, and a constant wavelength over the mirror. The existence of the wave was proof that the superfluid was free to oscillate. Observations of the well levels showed that transfer was still taking place at the high temperatures. Turning the chopper light off did not seem to increase this rate of transfer but

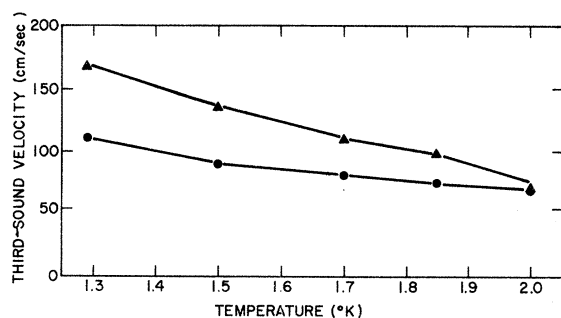


FIG. 10. Third-sound velocity versus temperature at  $l_1 = 5.4$  cm. It is seen that the downstream velocity is falling with temperature faster than the upstream velocity.

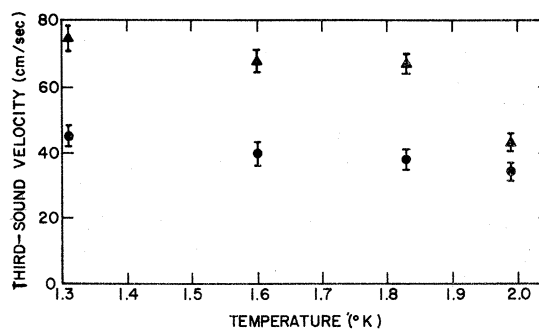


FIG. 11. Third-sound velocity versus temperature at  $l_1 = 1$  cm.

transfer rates are difficult to measure with this apparatus. However, the velocities of third sound measured at these temperatures were very much a function of chopper light intensity in contradiction to the low-temperature results which were independent of the light intensity. Cutting down on the light intensity tended to raise the downstream velocities and lower the upstream velocities, thus increasing the measured "critical velocity" at high temperatures. This suggests that plotting  $U_3$  down and  $U_3$  up against chopper-light intensity and extrapolating to zero intensity might give us the correct critical velocity. However, the extrapolated "critical velocity" is  $18 \pm 5$  cm/sec for a film height of 5.0 cm at  $1.92^\circ\text{K}$ . At  $1.2^\circ\text{K}$  the measured critical velocity for this film height is  $35 \pm 5$  cm/sec. Such a large drop in critical velocity as a function of temperature is inconsistent with all previous accepted transfer-rate measurements.

The dependence of the third-sound velocities on chopper intensity and the chopper decoupling of the film thickness from  $l_1$  dependence (which exists even at low temperatures) suggest that the excitation of the third-sound wave should be studied very carefully as the cause of these effects.

The infrared chopper radiation passes through the helium film with no losses and is reflected from the stainless-steel mirror at normal incidence. About 30% of the incident radiation is absorbed in the mirror. The penetration depth for infrared radiation in stainless steel is very small ( $\sim 10 \text{ \AA}$ ). Thus, a very thin slab of the mirror is heated directly. Some of the heat is conducted away by the metal, and the rest flows into the helium film. The ratio is difficult to determine because of the presence of a boundary thermal resistance (Kapitza resistance) at the interface between the film and mirror. The heat flowing into the film warms it locally to an amount  $\Delta T$  above the temperature of the vapor and the rest of the film. Two competing processes, an evaporation effect and the thermomechanical effect, then produce disturbances in the film sur-



face. The chopper light switches off and the film relaxes. The disturbances are propagated as a surface wave in the film. We deduce the nature of the chopper's effect on the film by studying the temperature differences and the energies necessary for production of a local 25% change in the film thickness (the observed amplitude) by each of the two processes. We will seek to determine what is responsible for the interference with the steady state (critical) flow of the film at high temperatures. Full details of the calculations are given in the thesis (see footnote to the title of this article). The results are summarized in Table I.

We see from the table that the situation is complicated by the competition of the two processes; it requires much more energy to make the evaporation process go but slightly less temperature elevation of the film. It should be noted that the two modes interfere destructively; a heat pulse tends to build a peak by the thermomechanical effect and a trough by the evaporation effect.

The ratio of heat flowing into the film to that dissipated in the metal is an important parameter because it tells us how much of the absorbed energy is available to perturb the film. We are especially interested in how this ratio changes with temperature. To determine this quantity we must know the surface impedance for heat flow (Kapitza resistance) from the metal to the film. An estimate is made which indicates that  $\sim 0.95$  of the available energy ( $2 \times 10^{-7}$  J) flows into the film at  $2.00^\circ\text{K}$  and  $\sim 0.75$  flows into the film at  $1.25^\circ\text{K}$ . These values are crude, but they indicate that the Kapitza resistance acts as a temperature dependent thermal valve allowing more heat to flow into the film at high temperatures.

We now ask what causes the film flow to apparently stop at high temperatures. Two possibilities are a dc thermomechanical effect drawing the film

towards the chopper and local heating above the  $\lambda$  point blocking the film flow. Consider again Fig. 4. If the film is heated sufficiently at the chopper region, it is possible for the film to flow out of  $l_1$  by the thermomechanical effect, even under the condition  $l_1 > l_2$ . Under these circumstances, the third-sound velocity measured would be an upstream velocity, independent of the relative magnitudes of  $l_1$  and  $l_2$ . We may calculate what temperature difference  $\Delta T$  must be set up to counteract the gravitational pressure head  $\Delta T = g/s \Delta H$ . For  $\Delta H = 0.5$  cm, we get

$$\Delta T = 7.5 \times 10^{-4} \text{ }^\circ\text{K} \text{ at } 1.25^\circ\text{K},$$

$$\Delta T = 5.5 \times 10^{-5} \text{ }^\circ\text{K} \text{ at } 2.00^\circ\text{K}.$$

Referring to Table I we see that these temperature differences are close to those calculated for the excitation of the wave. At high temperature the reduction of the Kapitza resistance shunts a greater portion of the heat into the film – more than the film can dissipate while the light is switched on. The heat decays slowly enough so that the film remains locally elevated in temperature during the  $\frac{1}{2}$  cycle the light is switched off. Thus, there is a dc flow towards the chopper region. The reasons this effect would occur at high temperatures are (a) the Kapitza resistance falls, giving more available heat, (b) it requires less of a temperature elevation to cause the dc thermomechanical effect at high temperatures, and (c) both modes of wave excitation require less heat and less temperature elevation at high temperatures to be effective and thus allow more heat to be available for the dc thermomechanical effect.

The experimental evidences for the existence of this effect are (1) the downstream third-sound velocity is affected more than the upstream velocity when the chopper light intensity is varied and (2) the downstream third-sound velocity falls

TABLE I. Results of calculations giving the necessary temperature elevations  $\Delta T$  and heat inputs  $Q$  required to produce film-thickness changes of 25% at temperatures of  $1.25^\circ\text{K}$  and  $2.00^\circ\text{K}$  in 2 msec ( $\frac{1}{2}$  a third-sound period) for the evaporation and thermomechanical disturbances. The evaporation parameters are derived from a consideration of the rate of evaporation for a given temperature elevation of the liquid over the vapor. For the thermomechanical disturbance, the most important factor is the amount of heat necessary to warm the superfluid flowing into the heated region. Included in the table is the experimentally observed incident infrared energy absorbed on the mirror. This is derived from a bolometer measurement of the chopper radiation absorbed in a carbon film corrected for the different reflectivities of carbon and stainless steel.

	Temperature ( $^\circ\text{K}$ )	Evaporation driven	Thermomechanically driven	Heat from chopper
$\Delta T$	1.25	$8 \times 10^{-5}$	$5 \times 10^{-4}$	
( $^\circ\text{K}$ )	2.00	$8 \times 10^{-5}$	$4 \times 10^{-5}$	
$Q$	1.25	$4 \times 10^{-7}$	$7 \times 10^{-10}$	
(J)	2.00	$4 \times 10^{-7}$	$6 \times 10^{-9}$	$2 \times 10^{-7}$

faster with temperature than the upstream third-sound velocity.

Another possible cause for the slowing down of the measured film velocity is the possible establishment of an abnormally high temperature in the chopper region. If the film is locally above the  $\lambda$  point, the flow will be stopped during part of the cycle. It is difficult to believe, however, that such large temperature differences can be set up in the film. We calculated that the evaporation mechanism, which is even more powerful at the high temperatures, would evaporate the film at temperature differences less than 1 mdeg while temperature elevations of greater than 0.1 deg would be needed. One would expect symmetry in the falling off with temperature of the upstream and downstream velocities if this mechanism were valid. As discussed above, we observe the downstream velocity falling faster.

#### E. Third Sound and Vortex Lines

Finally, the fact that third sound can exist in a static wave, and appear with such symmetry (see Enhancetron trace Fig. 2), should at first appear surprising. We are impressing a longitudinal wave on a film which is supposedly already moving at the highest velocity possible. One would expect that attempts to accelerate the film would only create dissipative vortices.

Let us consider the velocity along the mirror of a fluid particle. We assume it may be expressed as  $V_y = V_c + V_3$ , where  $V_3$  (not to be confused with  $U_3$ , the third-sound phase velocity) is the particle velocity due to third sound. According to theory,<sup>7</sup>

$$V_3 = V_0 \exp(i\omega t - ikx),$$

where  $V_0 = (\rho\delta_0/\rho_s d)U_3$ .

Here  $\delta_0$  is the amplitude of the wave and  $d$  is the film thickness.

Let us examine what happens to our measurements of the critical velocity as we increase  $V_0$ . We can accomplish this by increasing the intensity of the chopper light which will, in turn, increase  $\delta_0$ . Plotting the upstream third-sound velocity at the lowest temperature  $T=1.2^\circ\text{K}$  against the maximum third-sound amplitude as recorded on the tape, we get the results shown in Fig. 12. We see that  $U_{3\text{ up}}$  is independent of amplitude over a range of 7 in amplitude. The amount of heat necessary to attain the maximum amplitude can be taken from the data of Everitt *et al.* for a static film. This is obtained by plotting the wave amplitude versus the aperture area of the infrared focussing lens at the lowest temperature. The resulting curve is a straight line at small apertures (low intensities), which asymptotes to a constant amplitude at large apertures. We assume that this constant amplitude is equal to

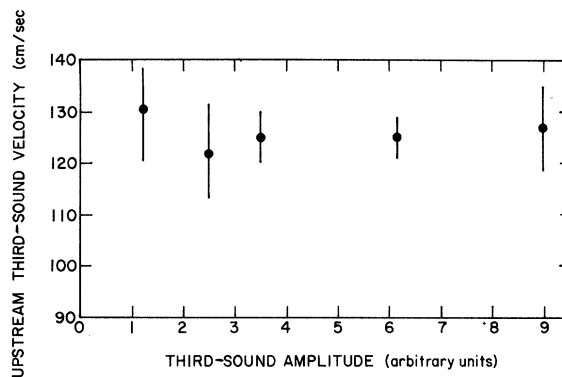


FIG. 12. Upstream third-sound velocity versus third-sound amplitude.

half the film thickness as indicated in Fig. 3 of Ref. 8 (this argues for the evaporation mechanism at least at low temperatures). The curve is independent of whether the film is static or in motion. The highest amplitude in Fig. 12 gives us  $\delta_0/d \sim 0.5$ . Calculating  $V_0$  from this by setting  $\rho/\rho_s = 1$  and  $U_3 = 165$  cm/sec, we see that  $V_0 \sim 80$  cm/sec. At this film height (9.0 cm) the critical velocity is 45 cm/sec. Thus the particle velocity is instantaneously twice the critical velocity. The particle velocity actually changes direction for a portion of the wave. (When critical velocity data were taken, the aperture was closed down so that  $\delta_0/d \sim 0.1$ .)

The best explanation for the existence of these hypercritical film velocities is that vortices cannot be created in the time  $T/2$  where  $T$  is the third-sound period. The longest period measured was  $\sim 20$  msec. Thus, we postulate that oscillatory behavior in a critically flowing film is possible as long as the time of the oscillation is less than  $\tau$ , a relaxation time for the formation of vortices and that  $\tau > 10$  msec.

#### V. CONCLUSION

We have measured the steady-state critical velocity of the liquid-helium film using third sound. The results lie very close to  $\hbar/2md$ . The thickness of a flowing film is determined from the data and is found to lie within 10% of that of the static film. Peculiar departures from expected results for the critical velocity as a function of pressure gradient and temperatures are explained as being due to the manner of excitation of the third-sound wave. A lower limit is placed on the time of formation of a steady-state vortex in the critically flowing film.

#### ACKNOWLEDGMENTS

We would like to acknowledge the preliminary work done on this experiment by Dr. C. W. F.

Everitt. We are indebted to Dr. R. Little for helpful discussions on the thickness of a moving film. A. Denenstein gave generous help with the

electronics design. P. Parkinson and Dr. A. Filler have aided this work with optical measurements.

\*Work supported by the National Science Foundation.

†Based on part of the thesis of Kenneth A. Pickar submitted in partial fulfillment of the requirements of the Physics Department for the degree of Doctor of Philosophy, University of Pennsylvania, 1966 (unpublished).

‡Now at Bell Telephone Laboratories, Murray Hill, New Jersey.

<sup>1</sup>L. C. Jackson and L. G. Grimes, *Advan. in Phys.* **1**, 435 (1958).

<sup>2</sup>K. R. Atkins, *Liquid Helium* (Cambridge University Press, Cambridge, England, 1959).

<sup>3</sup>K. R. Atkins, *Proc. Roy. Soc. (London)* **A203**, 240 (1950).

<sup>4</sup>J. G. Daunt and R. S. Smith, *Rev. Mod. Phys.* **26**, 172 (1954).

<sup>5</sup>W. C. Knudsen and J. R. Dillinger, *Phys. Rev.* **91**, 489 (1953); **95**, 279 (1954).

<sup>6</sup>J. R. Dillinger, *Conference de Physique des Basses Temperatures* (Supplement to Bull. Inst. Intern. Froid, p. 97, 1955).

<sup>7</sup>K. R. Atkins, *Phys. Rev.* **113**, 962 (1959).

<sup>8</sup>C. W. F. Everitt, K. R. Atkins, and A. Denenstein, *Phys. Rev.* **136**, A1494 (1964).

<sup>9</sup>I. Rudnick, R. S. Kagiwada, J. C. Fraser, and E. Guyson *Phys. Rev. Letters* **20**, 430 (1968).

<sup>10</sup>W. E. Keller and E. F. Hammel, *Phys. Rev. Letters* **17**, 988 (1966).

<sup>11</sup>For *unsaturated* [G. Kukich, R. P. Henkel, and J. D. Reppy, Proceedings of the Eleventh International Low-Temperature Conference, St. Andrews, Scotland, 1968 (to be published)] films  $v_c \rightarrow 0$  as  $d \rightarrow 0$ . However, this is probably due to the depression of the  $\lambda$  point in these films. Near the  $\lambda$  point  $v_c$  is known to go to zero.

<sup>12</sup>A. L. Fetter, *Phys. Rev.* **138**, 429 (1965).

<sup>13</sup>L. D. Landau, *J. Phys. (U. S. S. R.)* **5**, 71 (1941). A translation is found in the Appendix of I. M. Khalatnikov, *Introduction to the Theory of Superfluidity* (W. A. Benjamin, Inc., New York, 1965), p. 185.

<sup>14</sup>C. G. Kuper, *Nature* **185**, 831 (1960).

<sup>15</sup>V. M. Kontorovich, *Zh. Eksperim. i Teor. Fiz.* **30**, 805 (1956) [English transl.: *Soviet Phys. - JETP* **3**, 770 (1956)].

<sup>16</sup>R. Little, private communication.

<sup>17</sup>P. W. F. Gribbon and L. C. Jackson, *Can. J. Phys.*, **41**, 1047 (1963).

## Surface Waves on Bulk Liquid Helium\*†

K. A. Pickar‡ and K. R. Atkins

*Physics Department, University of Pennsylvania, Philadelphia, Pennsylvania*

(Received 30 September 1968)

The velocity of a surface wave on bulk liquid helium is measured as a function of frequency at temperatures above and below the  $\lambda$  point. The results do not reproduce those of Everitt, Atkins, and Denenstein. Below the  $\lambda$  point our results follow the classical theory, and no two-fluid effects are seen. There is some deviation from simple theory above the  $\lambda$  point. The variation in wave amplitude as a function of temperature is qualitatively consistent with the amplitude variation expected from consideration of the specific-heat curve.

### INTRODUCTION

The velocity of a surface wave on bulk liquid helium was first measured by Everitt, Atkins, and Denenstein.<sup>1</sup> They filled the inner chamber of their third-sound apparatus above the level of the stainless-steel mirror. A surface wave on

the resulting helium "puddle," which was  $\sim 0.1$  cm deep, was excited and detected by the same techniques used in the film work. The data at  $1.25^\circ\text{K}$  are shown in Fig. 1. The phase velocity  $V_p$  of a surface wave of a wavelength  $\lambda$  on an ideal classical liquid is given by<sup>2</sup>